

# Nanofocusing optics for synchrotron radiation made from polycrystalline diamond

O. J. L. Fox,<sup>1,2,\*</sup> L. Alianelli,<sup>1</sup> A. M. Malik,<sup>3,4</sup> I. Pape,<sup>1,5</sup> P. W. May,<sup>2</sup>  
and K. J. S. Sawhney<sup>1</sup>

<sup>1</sup>Diamond Light Source Ltd., Didcot, OX11 0DE, UK

<sup>2</sup>School of Chemistry, University of Bristol, Bristol, BS8 1TS, UK

<sup>3</sup>Micro and Nanotechnology Centre, Science and Technology Facilities Council, Didcot, OX11 0QX, UK

<sup>4</sup>Department of Engineering Science, University of Oxford, Oxford, OX1 3PJ, UK

<sup>5</sup>I. Pape is now with the Faculty of Engineering, University of Nottingham, NG7 2RD, UK

\*oliver.fox@diamond.ac.uk

**Abstract:** Diamond possesses many extreme properties that make it an ideal material for fabricating nanofocusing x-ray optics. Refractive lenses made from diamond are able to focus x-ray radiation with high efficiency but without compromising the brilliance of the beam. Electron-beam lithography and deep reactive-ion etching of silicon substrates have been used in a transfer-molding technique to fabricate diamond optics with vertical and smooth sidewalls. Latest generation compound refractive lenses have seen an improvement in the quality and uniformity of the optical structures, resulting in an increase in their focusing ability. Synchrotron beamline tests of two recent lens arrays, corresponding to two different diamond morphologies, are described. Focal line-widths down to 210 nm, using a nanocrystalline diamond lens array and a beam energy of  $E = 11$  keV, and 230 nm, using a microcrystalline diamond lens at  $E = 15$  keV, have been measured using the Diamond Light Source Ltd. B16 beamline. This focusing prowess is combined with relatively high transmission through the lenses compared with silicon refractive designs and other diffractive optics.

©2014 Optical Society of America

OCIS codes: (340.0340) X-ray optics; (220.3630) Lenses.

---

## References and links

1. G. E. Ice, J. D. Budai, and J. W. L. Pang, "The Race to X-ray Microbeam and Nanobeam Science," *Science* **334**(6060), 1234–1239 (2011).
2. L. Alianelli, K. J. S. Sawhney, R. Barrett, I. Pape, A. M. Malik, and M. C. Wilson, "High efficiency nanofocusing kinoform optics for synchrotron radiation," *Opt. Express* **19**(12), 11120–11127 (2011).
3. M. Sanchez del Rio and L. Alianelli, "Aspherical lens shapes for focusing synchrotron beams," *J. Synchrotron Radiat.* **19**(3), 366–374 (2012).
4. H. C. Kang, H. Yan, R. P. Winarski, M. V. Holt, J. Maser, C. Liu, R. Conley, S. Vogt, A. T. Macrander, and G. B. Stephenson, "Focusing of hard x-rays to 16 nanometers with a multilayer Laue lens," *Appl. Phys. Lett.* **92**(22), 221114 (2008).
5. K. Jefimovs, J. Vila-Comamala, T. Pilvi, J. Raabe, M. Ritala, and C. David, "Zone-doubling technique to produce ultrahigh-resolution x-ray optics," *Phys. Rev. Lett.* **99**(26), 264801 (2007).
6. C. David, S. Gorelick, S. Rutishauser, J. Krzywinski, J. Vila-Comamala, V. A. Guzenko, O. Bunk, E. Färm, M. Ritala, M. Cammarata, D. M. Fritz, R. Barrett, L. Samoylova, J. Grünert, and H. Sinn, "Nanofocusing of hard X-ray free electron laser pulses using diamond based Fresnel zone plates," *Sci. Rep.* **1**, 57 (2011).
7. E. Di Fabrizio, F. Romanato, M. Gentili, S. Cabrini, B. Kaulich, J. Susini, and R. Barrett, "High-efficiency multilevel zone plates for keV X-rays," *Nature* **401**(6756), 895–898 (1999).
8. A. A. Snigirev, V. Kohn, I. Snigireva, and B. Lengeler, "A compound refractive lens for focusing high-energy X-rays," *Nature* **384**(6604), 49–51 (1996).
9. V. Aristov, M. Grigoriev, S. Kuznetsov, L. Shabelnikov, V. Yunkin, T. Weitkamp, C. Rau, I. Snigireva, A. A. Snigirev, M. Hoffmann, and E. Voges, "X-ray refractive planar lens with minimized absorption," *Appl. Phys. Lett.* **77**(24), 4058–4060 (2000).

10. B. Nöhhammer, J. Hoszowska, A. K. Freund, and C. David, "Diamond planar refractive lenses for third- and fourth-generation X-ray sources," *J. Synchrotron Radiat.* **10**(2), 168–171 (2003).
11. K. Evans-Lutterodt, J. M. Ablett, A. Stein, C. C. Kao, D. M. Tennant, F. Klemens, A. Taylor, C. Jacobsen, P. L. Gammel, H. Huggins, G. Bogart, S. Ustin, and L. Ocola, "Single-element elliptical hard x-ray micro-optics," *Opt. Express* **11**(8), 919–926 (2003).
12. C. G. Schroer, O. Kurapova, J. Patommel, P. Boye, J. Feldkamp, B. Lengeler, M. Burghammer, C. Riekel, L. Vincze, A. van der Hart, and M. Küchler, "Hard x-ray nanoprobe based on refractive x-ray lenses," *Appl. Phys. Lett.* **87**(12), 124103 (2005).
13. L. Alianelli, K. J. S. Sawhney, M. K. Tiwari, I. P. Dolbnya, R. Stevens, D. W. K. Jenkins, I. M. Loader, M. C. Wilson, and A. M. Malik, "Characterization of germanium linear kinoform lenses at Diamond Light Source," *J. Synchrotron Radiat.* **16**(3), 325–329 (2009).
14. C. G. Schroer, M. Kuhlmann, J. Patommel, U. T. Hunger, T. F. Gunzler, O. Kurapova, S. Feste, M. Drakopoulos, A. Somogyi, A. S. Simionovici, A. A. Snigirev, I. Snigireva, C. Schug, and W. H. Schroder, "Nanofocusing parabolic refractive x-ray lenses," *Appl. Phys. Lett.* **82**(9), 1485–1487 (2003).
15. K. Evans-Lutterodt, A. Stein, J. M. Ablett, N. Bozovic, A. Taylor, and D. M. Tennant, "Using compound kinoform hard-x-ray lenses to exceed the critical angle limit," *Phys. Rev. Lett.* **99**(13), 134801 (2007).
16. C. G. Schroer and B. Lengeler, "Focusing Hard X Rays to Nanometer Dimensions by Adiabatically Focusing Lenses," *Phys. Rev. Lett.* **94**(5), 054802 (2005).
17. A. F. Isakovic, A. Stein, J. B. Warren, S. Narayanan, M. Sprung, A. R. Sandy, and K. Evans-Lutterodt, "Diamond kinoform hard X-ray refractive lenses: design, nanofabrication and testing," *J. Synchrotron Radiat.* **16**(1), 8–13 (2009).
18. L. Alianelli, K. J. S. Sawhney, A. M. Malik, O. J. L. Fox, P. W. May, R. Stevens, I. M. Loader, and M. C. Wilson, "A planar refractive x-ray lens made of nanocrystalline diamond," *J. Appl. Phys.* **108**(12), 123107 (2010).
19. A. A. Snigirev, V. Yunkin, I. Snigireva, M. Di Michiel, M. Drakopoulos, S. Kouznetsov, L. Shabel'nikov, M. Grigoriev, V. Ralchenko, I. Sychov, M. Hoffmann, and E. I. Voges, "Diamond refractive lens for hard X-ray focusing," *Proc. SPIE* **4783**, 1–9 (2002).
20. C. Ribbing, B. Cederström, and M. Lundqvist, "Microstructured diamond X-ray source and refractive lens," *Diamond Related Materials* **12**(10-11), 1793–1799 (2003).
21. A. M. Malik, O. J. L. Fox, L. Alianelli, A. M. Korsunsky, R. Stevens, I. M. Loader, M. C. Wilson, I. Pape, K. J. S. Sawhney, and P. W. May, "Deep reactive ion etching of silicon moulds for the fabrication of diamond x-ray focusing lenses," *J. Micromech. Microeng.* **23**(12), 125018 (2013).
22. O. Kurapova, B. Lengeler, C. G. Schroer, M. Küchler, T. Gessner, and A. van der Hart, "Optimized fabrication of silicon nanofocusing x-ray lenses using deep reactive ion etching," *J. Vac. Sci. Technol. B* **25**(5), 1626 (2007).
23. P. Boye, J. M. Feldkamp, J. Patommel, A. Schwab, S. Stephan, R. Hoppe, C. G. Schroer, M. Burghammer, C. Riekel, A. van der Hart, and M. Küchler, "Nanofocusing refractive X-ray lenses: Fabrication and modeling," *J. Phys. Conf. Ser.* **186**, 012063 (2009).
24. O. J. L. Fox, J. O. P. Holloway, G. M. Fuge, P. W. May, and M. N. R. Ashfold, "Electrospray Deposition of Diamond Nanoparticle Nucleation Layers for Subsequent CVD Diamond Growth," *MRS Proceedings*, **1203**, 1203–J17–27 (2009).
25. P. W. May and Y. A. Mankelevich, "From ultrananocrystalline diamond to single crystal diamond growth in hot filament and microwave plasma-enhanced CVD reactors: a unified model for growth rates and grain sizes," *J. Phys. Chem. C* **112**(32), 12432–12441 (2008).
26. J. C. Richley, O. J. L. Fox, M. N. R. Ashfold, and Y. A. Mankelevich, "Combined experimental and modeling studies of microwave activated CH<sub>4</sub>/H<sub>2</sub>/Ar plasmas for microcrystalline, nanocrystalline, and ultrananocrystalline diamond deposition," *J. Appl. Phys.* **109**(6), 063307 (2011).
27. J. E. Butler and I. Oleynik, "A mechanism for crystal twinning in the growth of diamond by chemical vapour deposition," *Philos Trans A Math Phys Eng Sci* **366**(1863), 295–311 (2008).
28. K. J. S. Sawhney, I. P. Dolbnya, M. K. Tiwari, L. Alianelli, S. M. Scott, G. M. Preece, U. K. Pedersen, R. D. Walton, R. Garrett, I. Gentle, K. Nugent, and S. Wilkins, "A Test Beamline on Diamond Light Source," *AIP Conf. Proc.* **1234**, 387–390 (2010).
29. V. V. Aristov, M. V. Grigoriev, S. M. Kuznetsov, L. G. Shabelnikov, V. A. Yunkin, M. Hoffmann, and E. Voges, "X-ray focusing by planar parabolic refractive lenses made of silicon," *Opt. Commun.* **177**(1-6), 33–38 (2000).
30. B. Lengeler, C. G. Schroer, J. Tümmeler, B. Benner, M. Richwin, A. A. Snigirev, I. Snigireva, and M. Drakopoulos, "Imaging by parabolic refractive lenses in the hard X-ray range," *J. Synchrotron Radiat.* **6**(6), 1153–1167 (1999).

---

## 1. Introduction

### 1.1 Synchrotron optics for nanofocusing

In recent years, the development of synchrotron and free-electron laser radiation sources, and their associated instrumentation, has allowed numerous flux-limited and coherence-dependent

x-ray experimental techniques to flourish. Hard x-ray beams of decreasing size and increasing flux and coherence allow experiments in chemistry, biology, material science and physics to take place which would be unthinkable within a standard laboratory. Examples include structure determination in protein crystallography, phase imaging of low-density materials, time-resolved experiments, nanocrystal studies, and lens-less imaging [1].

The successful design and installation of synchrotron beamlines relies on the availability of near-perfect optics for the monochromatisation, collimation and focusing of the radiation. Curved focusing optics (mirrors and refractive lenses) must possess extremely well-defined shapes with minimal figure errors in order to prevent aberrations, degradation of the beam uniformity and flux losses [2,3]. In-line nanofocusing optics, such as multilayer-Laue lenses [4] and zone plates [5–7], can currently be fabricated which have sub-mm sizes and smallest features < 10 nm.

Refractive optics, widely used for focusing x-rays, exist in two general lens designs. Compound refractive lenses (CRLs) consist of arrays of parabolic or elliptical surfaces where each lens element in turn focuses the x-ray beam with a short focal length, despite the small decrement of refractive index of x-rays in most media [8]. However, the large volume of material through which the beam passes leads to significant absorption, and aberrations can arise as the transmitted radiation is refracted by each lens element in the array. In contrast, kinoform lenses focus x-rays with a shorter path length of radiation within the lens by removing phase-neutral material [9–11]. This results in a reduction in the inherent absorption and scattering of the beam. Nanofocusing CRLs and kinoforms are commonly planar optics that only focus in one dimension, although a point focus can be achieved by using two lenses in a crossed geometry [12,13].

Compound refractive [14] and kinoform lenses [2,11,15] manufactured from single crystal silicon with vertical walls only 2 – 4  $\mu\text{m}$  thick have been produced. However, the flux and effective aperture of silicon refractive lenses are absorption limited [15]. In the case of x-ray nanofocusing zone plates, the fabrication of high-aspect-ratio structures proves difficult and leads to a limitation in device efficiency above  $E = 10$  keV. Zone plates and silicon compound refractive or kinoform lenses perform excellently for many nanofocusing experiments but there is a requirement for optics, with low absorption (high efficiency) and short focusing distances, that function in high-power-density x-ray beams.

### 1.2 Refractive lens design

Focusing and absorption of x-rays in the lens material is described by the refractive index:

$$n = 1 - \delta + i\beta$$

where  $\delta$  is the refractive index real-part decrement given by:

$$\delta = f_1 \frac{r_0 \lambda^2}{2\pi} \frac{N_A}{A} \rho \approx Z \frac{r_0 \lambda^2}{2\pi} \frac{N_A}{A} \rho.$$

In the previous equation  $f_1$  is the real part of the atomic scattering factor and can be approximated by the atomic number  $Z$  for energies above 1 keV,  $r_0$  is the classical electron radius,  $\lambda$  is the wavelength of the incident x-rays,  $N_A$  is Avogadro's number,  $A$  is the atomic mass and  $\rho$  is the material density.  $\beta$  is the absorption index and describes the attenuation (absorption and scattering caused by photoelectric effect, Compton effect and pair-production) of x-rays in matter, via the absorption coefficient,  $\mu$ :

$$\beta = \frac{\lambda\mu}{4\pi}$$

The refractive index real-part decrement  $\delta$  is a very small number ( $\sim 10^{-5} - 10^{-6}$ ) and, therefore, hard x-ray lenses are designed and fabricated with a very pronounced curvature, following a conic section [3]. A nanofocusing lens made of a single focusing element is not

feasible, due to the required curvature, and so, in the CRL design, x-ray optics are often made using arrays of conical surfaces. X-ray lens apertures are small due to both fabrication issues and non-negligible absorption and, therefore, the focal length of the CRL arrays is described in good approximation by the thin lens formula:

$$f = \frac{R}{N\delta}$$

where  $f$  is the focal length,  $R$  is the radius of curvature at the apex of the refractive surfaces and  $N$  is the number of refractive surfaces. CRLs exist in several designs with typical low-aberration refractive optics made using conical surfaces, such as Descartes' ovals, ellipses and hyperbolas [3]. Due to the small aperture and relatively large radius  $R$  of the lenses, the design chosen here (parabolic arrays with  $N = 6 - 80$  and  $R = 25 \mu\text{m}$ ) creates minimal geometrical aberrations. It has been verified by ray-tracing methods that such aberrations do not broaden the focused beam significantly.

Achieving single-digit nanometer sized focused beams with refractive lenses is theoretically possible [15,16]. Therefore, advances in micro-fabrication using both silicon and diamond technologies would deliver an x-ray optic with unprecedented brilliance.

### *1.3 Nanofocusing lenses made from diamond*

Nanofocusing optics made from diamond allow improved thermal load management, due to its high thermal conductivity and low thermal coefficient of expansion, and provide greater transmission efficiencies due to the lower photoelectric absorption compared with higher  $Z$  materials. Indeed, the resilience of diamond to the intense radiation and thermal loads produced at fourth-generation x-ray sources makes it one of the few materials able to operate stably under such conditions.

Although excellent quality single crystal diamond devices have been characterized in detail using x-rays, and are routinely used as synchrotron monochromators, polarizers, beam splitters, windows and radiation detectors, the current unavailability of large, uniform single crystal substrates limits their use as refractive lenses, which typically require substrate dimensions  $> 10 \text{ mm}$ . While single crystal diamond provides the ideal material for fabricating x-ray nanofocusing optics, alternative lenses have successfully been produced by plasma etching of polycrystalline diamond films [10,17]. Unlike the single crystal material, the diamond grains making up the polycrystalline material will scatter x-rays to some extent, dependent on the distribution of particle sizes. Materials with grain diameters in the range  $1 - 5 \mu\text{m}$  are termed microcrystalline diamond (MCD) and those with grains  $< 100 \text{ nm}$  are nanocrystalline diamond (NCD). Etching polycrystalline diamond suffers from a number of drawbacks, such as the diamond etch uniformity, high surface roughness and poor sidewall verticality, which can severely compromise lens performance, as well as slow etch rates, which increase fabrication time prohibitively.

To overcome these issues, current silicon microfabrication techniques, including electron-beam lithography and deep reactive-ion etching (DRIE), offer alternative solutions for fabrication of high-resolution synchrotron optics for nanofocusing experiments [2]. These same methods have been used to fabricate high-quality silicon molds into which polycrystalline diamond is deposited to produce x-ray focusing compound refractive [18] and kinoform [19] lenses.

### *1.4 Diamond refractive optics using silicon-mold microfabrication*

Fabrication of refractive diamond optics using transfer molding involves deposition of polycrystalline diamond onto high-quality silicon templates using microwave-activated plasma chemical vapor deposition (MWCVD). After filling of the template, the structures are bonded to 30 mm diameter, 1 mm thick, diamond handling substrates and the silicon layer is

removed using a plasma etch to reveal the diamond lens structures [18,20]. Filling of the Si mold is achieved with high fidelity so that parameters such as surface smoothness and sidewall verticality, of crucial importance in the fabrication of x-ray nanofocusing lenses, are determined by the silicon template rather than by the diamond deposition. The etch and passivation cycle times of the Bosch process used to etch the silicon molds have been optimized to produce high-aspect-ratio structures with vertical sidewalls [21 and references therein]. Consequences on the lens focusing of errors in the lithography pattern transfer and a non-ideal (*i.e.*  $\neq 90^\circ$ ) etch angle for silicon lenses have been quantified previously [22,23]. Steady progress is being made in the field of silicon etch by Bosch and cryogenic techniques, as reduced surface scalloping and etch angles close to  $90^\circ$  are obtained.

The initial nanocrystalline diamond CRLs were tested on the B16 beamline at the Diamond Light Source Ltd. synchrotron and achieved focal widths (FWHM in one plane) of  $1.6 \mu\text{m}$  (at  $E = 12 \text{ keV}$  and a focal length of  $f = 0.56 \text{ m}$ ) [18]. Improvement in the lens design and the diamond deposition step in the second iteration of CRLs allowed a FWHM of  $400 \text{ nm}$  to be achieved (at  $E = 11 \text{ keV}$  and  $f = 0.19 \text{ m}$ ) [21]. Recent advances in the selected-area nucleation of diamond layers and the increasing stability of nanofocusing experiments on the B16 beamline have led to a further reduction in the focal widths, and the results from both nano- and microcrystalline diamond CRL structures are discussed here.

## 2. Experimental

### 2.1 Mold fabrication

Silicon molds were fabricated from  $100 \text{ mm}$  diameter,  $500 \mu\text{m}$  thick  $\langle 100 \rangle$  wafers using optical lithography ( $2 \mu\text{m}$  spin-coated SU8-2 photoresist,  $3 \text{ s}$  UV exposure (MA6, SUSS MicroTec Lithography) and  $60 \text{ s}$  develop with EC solvent from Rohm and Haas Electronic Materials). The DRIE step was carried out in an inductively coupled plasma etcher (Surface Technology Systems) using the Bosch process [21]. Device wafers were diced into nine  $20 \times 20 \text{ mm}$  lens chips using laser machining (Alpha, Oxford Lasers). Each lens chip carried 16 CRL arrays designed to focus a range of x-ray wavelengths ( $E = 5 - 20 \text{ keV}$ ) with a focal length of  $f = 50 \text{ mm}$ . This flexibility within one lens chip allows the focusing ability of the optic to be assessed relatively easily at a number of different beam energies by translating the lens chip in the beam.

A schematic diagram and electron microscope image of the CRL design is shown in Figs. 1(a) and 1(b), respectively. The geometrical aperture of a typical lens is  $A = 200 \mu\text{m}$  in one plane and  $D \approx 30 \mu\text{m}$  in the perpendicular plane, the latter governed by the thickness of the diamond film within the mold.

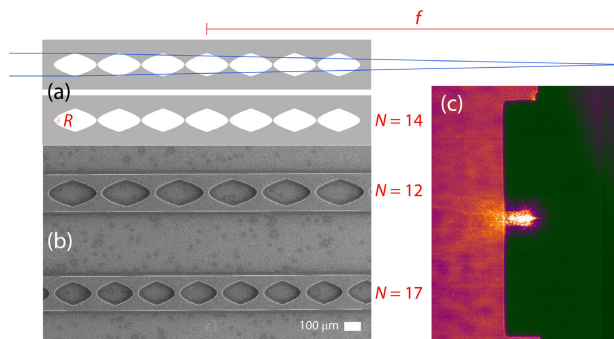


Fig. 1. (a) Schematic diagram of the CRL design showing two arrays of  $N = 14$  concave surfaces with radius of curvature  $R$  and focusing the incident beam with a focal length  $f$ . (b) SEM image of part of a CRL chip showing two further lens arrays designed to focus x-ray radiation of different wavelengths. (c) Wide-angle image from B16 beamline detector showing the line focus from the CRL and associated scattering.

## 2.2 Lens fabrication

For the heteroepitaxial growth of diamond onto the silicon molds a nucleation layer was required. This was applied in two stages: firstly, a selected-area nucleation step seeded only the recessed regions of the mold using solution-based self-assembly of diamond nanoparticles onto the silicon surface and, secondly, by electrostatic spraying of diamond nanoparticles (suspended in methanol) onto the entire mold [24]. Following seeding, diamond was deposited onto the silicon molds using a 2.45 GHz MWCVD reactor under conditions chosen to achieve the desired crystalline morphology at a suitably high rate of deposition [25,26]. Optimized conditions, chosen to produce uniform diamond films at a reasonable growth rate, typically involved deposition in methane/hydrogen plasmas ( $\sim 7\%$   $\text{CH}_4$  in  $\text{H}_2$ ) with input MW power of  $P = 1$  kW and chamber pressure of  $p = 110$  Torr for between 12 – 18 h at a substrate temperature of  $T_{\text{sub}} = 1000$  K. Control of the crystalline morphology was possible by addition of a small amount ( $<1\%$ ) of  $\text{N}_2$  to the plasma [27]. This allowed fabrication of diamond lens structures of either a nanocrystalline (with crystal sizes  $\sim 50$  nm) or microcrystalline ( $\sim 1 - 2$   $\mu\text{m}$ ) texture with little variation in the plasma conditions and deposition rate.

After diamond deposition, the diamond lens chips were bonded to 30-mm-diameter CVD diamond handling substrates (Element Six Ltd.) and the silicon mold was removed from the back surface using a plasma etch to expose the diamond lens arrays in relief. Thick diamond handling substrates were used to provide a good thermal contact with the lens and reduce any thermally-induced stress occurring when the optic was exposed to high-power-density beams. The form fidelity and surface roughness of diamond optics fabricated using the transfer-molding approach is apparent in electron microscope images (Fig. 2).

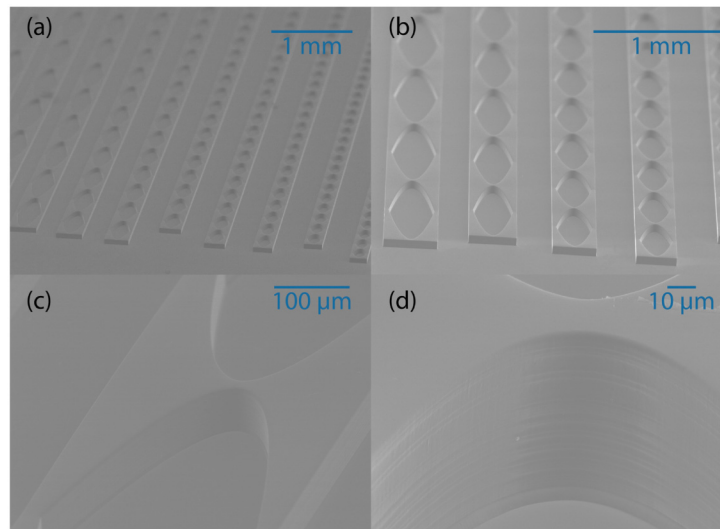


Fig. 2. Tilted-SEM images showing diamond CRL structures with increasing magnification from (a) to (d). The absence of extraneous structures around the lenses is apparent in (a) and (b) and the remarkable form fidelity of the silicon-diamond transfer molding process is clear in (c) and (d), where the scalloped surface deriving from the silicon etch is observed.

## 2.3 Optic testing on B16 beamline

Lens substrates prepared for testing were mounted in a vertical focusing geometry in the x-ray beam on the B16 test beamline at the Diamond Light Source synchrotron as detailed in previous work [2,18,28]. The beamline layout included a double bounce single crystal silicon  $\langle 111 \rangle$  monochromator and slit system that delivered a monochromatic beam, of controlled spatial dimensions, to the CRL under investigation. The CRL was located at a distance  $p = 47.189$  m from the bending-magnet source and exposed to radiation with energies of

$E = 11 - 19$  keV. The diagnostic system consisted of a high-spatial-resolution detector, based on a  $5\ \mu\text{m}$  europium-doped lutetium aluminum garnet ( $\text{Lu}_3\text{Al}_5\text{O}_{12}$ ) scintillator, a microscope and a PCO4000 CCD camera. Focal widths produced by the CRL were measured by scanning a  $200\ \mu\text{m}$  gold wire in the focal plane using a piezoelectric system. The resulting change in intensity as the wire intersected the beam was recorded using a calibrated photodiode (Fig. 3). Differentiation of this intensity signal produced a focused beam profile from which a FWHM was extracted.

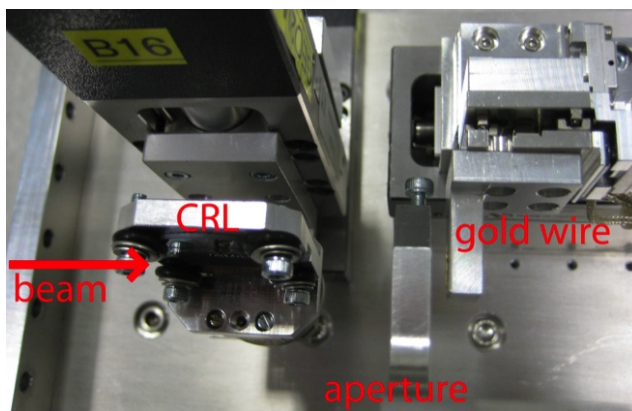


Fig. 3. Nanofocusing setup on the B16 beamline at the Diamond Light Source showing the x-ray beam propagating from left to right, the CRL mounted in vertical orientation, mounting for the  $30\ \mu\text{m}$  anti-scatter aperture and the gold-wire knife-edge situated on positioning stages.

Construction of a stable nanofocusing platform has also led to improvements in the focusing measurements on the B16 beamline. The platform allows precision alignment of the lenses and scanning of the gold-wire knife-edge each in 6 degrees-of-freedom. To remove some of the contribution from small-angle x-ray scattering (SAXS) either anti-scatter slits ( $50\ \mu\text{m}$ ) or an orifice ( $30\ \mu\text{m}$ ) were positioned between the CRL and the gold wire.

It is important to note that two of the focusing experiments (Table 1: D & E) were conducted with the DLS synchrotron operating in low-emittance mode. In all other measurements the machine operated with 1% vertical coupling whereas in low-emittance mode this coupling was reduced to 0.3% with the advantages of a smaller vertical source size and greater spatial coherence. In reducing the coupling from 1% to 0.3% the vertical source size was halved, from the nominal  $\sigma_{\text{source}} = 56\ \mu\text{m}$  to  $\sigma_{\text{source}} = 28\ \mu\text{m}$ . As there is no decrease in the photon beam divergence when operating with low coupling the photon flux density does not increase. Working in a low-emittance mode is desirable for nanofocusing and coherence experiments and will have aided the achievement of narrow focusing observed for these two experiments.

### 3. Results and discussion

#### 3.1 Optical quality and testing

Advances have been made to both the mold fabrication and the diamond deposition in this latest iteration of nanofocusing optics. A reduction in the lens surface roughness has been achieved by optimizing the DRIE step to minimize the scalloping deriving from the Bosch process etch-and-passivation cycles [21]. Improvement in the selected-area nucleation of the silicon molds with nanodiamond particles has allowed thicker diamond layers to be deposited and greater uniformity across the substrate. Taken together, these developments have resulted in the fabrication of a more homogenous diamond optic.

Radiation scattered by the lenses comes from either surface scattering due to the DRIE scalloping and surface inhomogeneity or from internal scattering from defects and grain



boundaries in the polycrystalline material. To investigate the effect of crystallite size, both microcrystalline and nanocrystalline diamond CRL chips were fabricated, the former using a H<sub>2</sub>/CH<sub>4</sub>/Ar CVD plasma and the latter with a H<sub>2</sub>/CH<sub>4</sub>/N<sub>2</sub> plasma. SAXS by the lenses, and its contribution to the focal width and transmission efficiency, could then be assessed as a function of diamond morphology. Although the surface scalloping has been reduced, it has not been completely eliminated so some scattering results from the surface roughness of the lens. A study of the relationship between the SAXS contribution to the measured focal intensity and the diamond morphology (grain size, grain boundaries and defects) will be the subject of a future publication.

Analyzing the phase content of the lens material by x-ray powder diffraction and UV-Raman scattering before and after long exposures to the synchrotron radiation showed only diamond phases and no graphitization of the sample. Inclusion of silicon or metal atom contaminants within the lens is more important for x-ray applications than the presence of amorphous phase carbon at the boundary between diamond grains. However, compositional analysis of the diamond material using secondary ion mass spectrometry and x-ray photoelectron spectroscopy indicates that concentrations of these trace elements are negligible in the CVD material.

### 3.2 Nano- and microcrystalline diamond CRLs

In the latest iteration of lenses, improved control of the silicon etch, the nucleation of the diamond layer and the filling of the mold has resulted in a CRL performance that was significantly better than previous tests. The x-ray image (Fig. 1(c)) was obtained by illuminating the lens with a wide beam as part of the alignment process and shows the linear focus with minimal extraneous light coming from the optic (as had been observed in previous iterations [18]) although the scattering surrounding the line focus is immediately apparent.

A comparison of the most recent focusing results from the B16 beamline (D – H) with previous iterations (A – C) is made in Table 1. All lenses were able to focus the x-ray beam from the bending magnet source to a well-defined line focus of micrometer or sub-micrometer size without creating any unwanted satellite structures. Each successive generation has seen an improvement in the focusing ability and a decrease in the focal width [18,21]. The diffraction limit,  $\sigma_{diff}$ , in Table 1 has been calculated using the following formula:

$$\sigma_{diff} = 1.22 \frac{\lambda}{NA}$$

where  $\lambda$  is the wavelength of the incident x-rays and  $NA$  is the numerical aperture given by:

$$NA = \frac{A}{f}$$

and  $A$  lens illuminated aperture. The source geometrical demagnification is defined as:

$$\sigma = \sigma_{source} \frac{q}{p}$$

with:

$$\frac{1}{f} = \frac{1}{p} + \frac{1}{q}$$

The theoretical beam size is a convolution of geometrical demagnification ( $\sigma$ ) and diffraction ( $\sigma_{diff}$ ) effects.  $p$  is the distance from the x-ray source to the centre of the lens and  $q$  is the distance from the center of the lens to the focal spot.



**Table 1. Summary of CRL Focusing tests where the Lenses were Used to De-magnify the Bending-magnet Source at B16 in the Vertical Plane**

Lens	Diamond	$E$	$f$	$\sigma$	$\sigma_{diff}$	Theoretical focus	Measured beam	Reference	
		[keV]	[m]	[nm]	[nm]	FWHM	FWHM		
						[nm]	[nm]		
A	NCD	18	1.06	1273	88	1276	2200	[18]	
B	NCD	12	0.56	667	122	678	1600	[18]	
C	NCD	11	0.19	238	109	262	900	[21]	
C*	NCD	11	0.19	238	91.4	255	400	[21]	
D	NCD	11	0.06	36	74	82	210	Fig. 4(a)	
E	MCD	15	0.05	30	51.5	59	230	Fig. 4(b)	
F	MCD	15	0.05	59	51.5	79	370	Fig. 4(c)	
G*	MCD	15	0.05	59	51.5	79	350	Fig. 4(d)	
H	MCD	19	0.05	59	54	80.5	900	-	

Note on Table 1: The results for lenses C\* and G\* were obtained by placing an anti-scatter orifice between the lens and the diagnostics wire. Lenses D and E were tested with the DLS synchrotron operating in a low-coupling mode providing a nominal source size of  $\sigma_{source} = 28 \mu\text{m}$  in the vertical plane. The effective source size for the other tests was  $\sigma_{source} = 56 \mu\text{m}$ . The calculated source demagnification,  $\sigma$ , diffraction limit,  $\sigma_{diff}$ , and theoretical focal FWHM for each lens and focusing geometry are also shown.

Most recently (Table 1, D), a nanocrystalline diamond CRL designed to focus at  $E = 11$  keV and  $f = 0.06$  m was tested with the DLS synchrotron operating in low-coupling mode, and achieved the narrowest FWHM yet measured. The results in Fig. 4(a) show a line focus FWHM of 210 nm using an illuminated aperture of  $20 \times 80 \mu\text{m}$ . The signal from a microcrystalline diamond lens (Table 1, E) working at  $E = 15$  keV and  $f = 0.05$  m is much higher and achieved a similar focal width, FWHM = 230 nm, with the machine in low-coupling mode, Fig. 4(b). Hence, broadening of the focus appears not to be dominated by the x-ray scattering from the diamond morphology because the crystal size of the NCD and MCD lenses is starkly different while the focusing results are roughly equivalent. X-ray beams from synchrotron sources are typically modeled using Gaussian profiles. However, imperfections in the focusing optics and vibrations in the beam mean that experimental focal profiles from silicon and diamond lenses are often fitted with Lorentzian curves as shown in Fig. 4. Further investigation will indicate whether the broadening of the focus away from the theoretical width is due to the surface roughness, the lens design or the diamond material.

Other results using the microcrystalline CRL were obtained at normal-coupling mode (Table 1, F–G). Working at  $E = 15$  keV and  $f = 0.05$  m, these results showed a line focus FWHM of 370 nm (Fig. 4(c)) and 350 nm with an anti-scatter orifice between lens and detection wire (Fig. 4(d)). While this could not match the 210 nm FWHM achieved with the NCD lens at low-coupling mode, the increase in the intensity at the focus gave better resolution above the background noise level. No unwanted satellite or diffraction peaks were observed for the MCD lens tests and this material may prove superior for fabrication of lens optics in future. At higher energy ( $E = 19$  keV), the small-angle x-ray scattering by the lens broadens the focused image (Table 1, H) and a FWHM of 900 nm was observed for the same focal length. A wide depth of focus has been measured for these lenses, indicating that background intensity is present broadening the focal spot. If diamond optics are to be utilised on higher-energy x-ray beamlines then this broadening will need to be addressed by improving the lens surface, limiting scattering from the diamond material and reducing the path length of the beam within the lens.

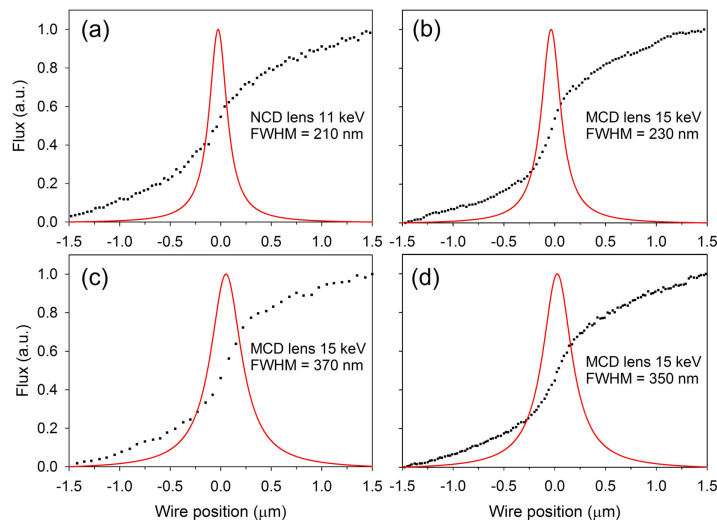


Fig. 4. Focusing results for 4 CRL lenses on the B16 beamline made using a gold-wire knife-edge method. Plots show normalized intensity measured by the detector (black dots) and Lorentzian fitting curves of the derivative (*i.e.* the beam profile; red line) for (a) NCD lens at  $E = 11$  keV and low-coupling mode, (b) MCD lens at  $E = 15$  keV and low-coupling mode, (c) MCD lens at  $E = 15$  keV and normal-coupling mode and (d) MCD lens at  $E = 15$  keV with anti-scatter aperture and normal-coupling mode. Illuminated apertures ( $x_A \times y_A$ ) were (a)  $20 \times 80$   $\mu\text{m}$ , (b)  $30 \times 80$   $\mu\text{m}$ , (c)  $20 \times 80$   $\mu\text{m}$  and (d)  $35 \times 80$   $\mu\text{m}$ , where  $x_A$  is the horizontal aperture and  $y_A$  is the vertical aperture.

For the NCD lens, a deviation of the measured focal length from calculated values was observed, with typical measured focal lengths being 10% – 15% longer than the theoretical values. This is likely to be due to a slightly lower density of the nanocrystalline material that contains a higher proportion of amorphous carbon than the microcrystalline morphology.

### 3.3 Transmission through the lenses

Lens efficiencies were determined by comparing the intensity of the focused beam with the incident beam (*i.e.* with no lens in the beam) for a range of geometrical apertures [29]. For planar refractive optics the effective aperture is defined as the aperture that transmits 75% of the full flux from the lens, and is typically smaller than the total aperture. As previously observed [18], the effective aperture for the diamond CRLs is larger ( $\sim 80 - 90$   $\mu\text{m}$ ) than those in absorption-limited silicon nanofocusing optics.

The transmission characteristics for four CRL arrays are shown in Fig. 5 together with theoretical calculations of the lens efficiencies [30]. In general, lens efficiency is reduced for wider apertures due to the increased absorption as a greater proportion of the lens is illuminated. The experimental results are proportional to the calculated values and deviation can be ascribed to scattering from both the polycrystalline diamond bulk material and the scalloped lens surface. The experiment is not able to completely distinguish beam intensity from either scattering source and the intensity in the focal spot.

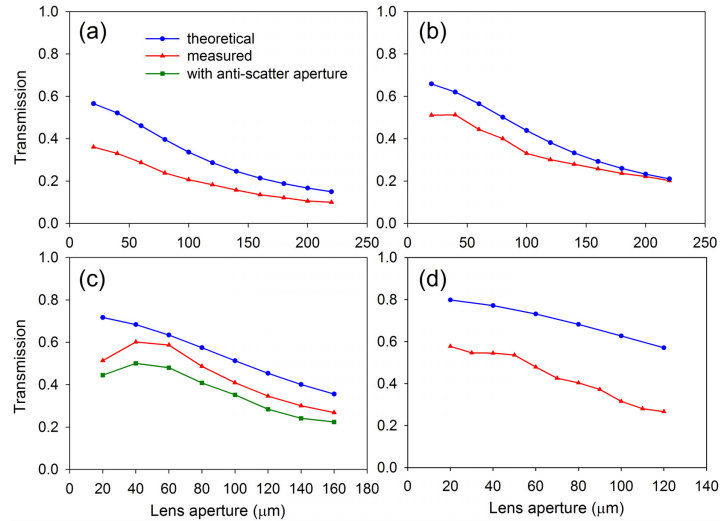


Fig. 5. Theoretical and measured lens efficiencies at different vertical apertures ( $y_A$ ) for 4 CRL lenses. (a) NCD lens at  $E = 11$  keV, (b) MCD lens at  $E = 14$  keV, (c) MCD lens at  $E = 15$  keV with and without anti-scatter orifice and (d) MCD lens at  $E = 19$  keV. Horizontal aperture  $x_A = 20$   $\mu\text{m}$ .  $f = 0.06$  m for the NCD lens (a) and  $f = 0.05$  m for the MCD lenses (b) – (c). Measured transmission efficiencies are derived from the ratio of focused x-ray intensity to incident flux. Theoretical transmission values assume a diamond density of  $3.5$   $\text{g cm}^{-3}$ . Note the varying scale on the horizontal axis.

Lens efficiency increases with both diamond grain size and x-ray energy although scattering losses are most pronounced at shorter wavelengths (Fig. 5(d)). When an anti-scatter aperture is positioned between the lens and the detector a further reduction in transmission is observed (Fig. 5(c)) indicating that the orifice cuts off some of the x-ray beam. The drop in efficiency at apertures  $< 50$   $\mu\text{m}$  for this CRL is not easily explained. It suggests that a larger portion of the incident flux is scattered rather than focused when using a smaller aperture, possibly due to a lens defect along its central axis. Quantification of this effect would require a complex modeling of SAXS, diffraction and focusing by the lens, including a possible material defect. Performing a measurement or simulation of the efficiency drop caused by SAXS and surface roughness would be of great interest. This would require design and fabrication of structures with the same amount of MCD or NCD material as that traversed by the x-ray beam in the transmission measurements. Finally, for the microcrystalline diamond lens working at  $E = 14$  keV the measured transmission comes closest to the theoretical values whereas a deviation is observed for higher energy x-rays ( $E = 15$  or  $19$  keV) or smaller crystallite sizes (NCD lens).

Observed CRL efficiencies compare well with other in-line nanofocusing, short-focal-length optics, especially those made from silicon and higher-atomic-mass materials. Taking two lenses in a crossed geometry to achieve a point focus requires multiplication of the efficiency in one plane. Some intensity values at the focus using the theoretical and experimental transmission results in Fig. 5 are shown in Table 2 for a nominal undulator beamline source with incident flux of  $1 \times 10^{12}$  photons  $\text{s}^{-1} \text{mm}^{-2}$ , in an energy bandwidth of  $\Delta E/E = 10^{-4}$ , and an illuminated aperture of  $50 \times 50$   $\mu\text{m}$  (assuming a  $> 50$ - $\mu\text{m}$ -deep mold can be adequately filled with diamond). Focal spot flux values  $> 2 \times 10^8$  photons  $\text{s}^{-1}$  are highly desirable for many nanofocusing applications at synchrotron sources and indicate an advantage of diamond optics over zone-plate optics focusing that provide superior demagnification but with a large loss in beam intensity.

**Table 2. Predicted Beam Flux after the Nanofocusing Optic for Crossed CRLs on an Undulator Beamline with a Source Intensity of  $1 \times 10^{12}$  Photons  $s^{-1} mm^{-2}$  and an Illuminated Aperture of  $50 \times 50 \mu m$  based on theoretical and experimental Transmission Measurements in Fig. 5**

Lens	Diamond	$E$ [keV]	Theoretical Flux [photons $s^{-1}$ ]	Predicted Flux [photons $s^{-1}$ ]
D	NCD	11	$6.0 \times 10^8$	$2.4 \times 10^8$
-	MCD	14	$8.8 \times 10^8$	$5.7 \times 10^8$
G*	MCD	15	$1.1 \times 10^9$	$6.0 \times 10^8$
H	MCD	19	$1.4 \times 10^9$	$7.2 \times 10^8$

The average pathlength of the x-ray beam within a kinoform lens structure is shorter than within a CRL. Achievement of x-ray nanofocusing below 50 nm with diamond refractive lenses made using the transfer-molding technique will be possible in the near future by utilizing the kinoform design, resulting in optics with higher transmission and reduced SAXS.

### Conclusions

Micro- and nanocrystalline diamond x-ray nanofocusing lenses have been successfully fabricated using a novel deposition technique allowing accurate control of the surface roughness and material morphology. Beamline tests have achieved focusing results down to 230 nm FWHM for a MCD lens and 210 nm for a NCD lens and the narrowest focal widths were observed with the DLS synchrotron operating in a low-coupling mode. As well as decreasing the focal width in each iteration of these planar in-line optics, high transmission values have been measured for a range of lenses, x-ray energies and illuminated apertures. This has indicated that the flux at a point focus provided by a pair of crossed CRLs on an undulator beamline could be greater than  $10^8$  photons  $s^{-1}$ . A reduction in the scattered light due to the diamond material, the surface roughness and lens aberrations in future optics will produce even higher flux and smaller focal spots.

### Acknowledgments

The Science and Technology Facilities Council (UK) Technology Department are acknowledged for providing funding for diamond lens development through the Centre for Instrumentation. This work was undertaken on beamline B16 at Diamond Light Source under proposal number NT5870.